

The Structural Dynamic Evaluation of Wadaslintang Dam to the Earthquake Acceleration Based on Indonesian Seismic Code 2019

Dwi Astuti Wahyu Wulan Pratiwi¹, Lalu Makrup¹, Imam Setiawan²

¹Department of Civil Engineering, Islamic University of Indonesia, Yogyakarta, Indonesia

²Earthquake Study Group, Islamic University of Indonesia, Yogyakarta, Indonesia

Email address:

lalu_makruf@yahoo.com (L. Makrup), 885110106@uii.ac.id (L. Makrup)

To cite this article:

Dwi Astuti Wahyu Wulan Pratiwi, Lalu Makrup, Imam Setiawan. The Structural Dynamic Evaluation of Wadaslintang Dam to the Earthquake Acceleration Based on Indonesian Seismic Code 2019. *American Journal of Civil Engineering*.

Vol. 10, No. 3, 2022, pp. 125-134. doi: 10.11648/j.ajce.20221003.15

Received: May 17, 2022; **Accepted:** June 10, 2022; **Published:** June 20, 2022

Abstract: Dam evaluation needs to be carried out, to look back at the deformation of the dam structure during decades of operation. In this study, the structure of Wadaslintang dam will be evaluated based on dynamic earthquake loading on the basis of the 2019 Indonesian earthquake hazard map. Dynamic evaluation of the dam requires dynamic earthquake acceleration in the form of a acceleration time history that was developed deterministically. Based on the theory of dam or soil deformation that was formatted in the GEOSTUDIO computer program and the program used in this research with the soil and earthquake time history data, so the deformation of the Wadaslitang dam can be computed. From the computation results can be stated that the dam safe to deformation. The result of the Wadaslitang dam evaluation was the vertical and the horizontal deformation has smaller deformation than the set requirement.

Keywords: The Ground Motion, Time History, Deterministic, Dam Structure Response

1. Introduction

Wadaslintang Dam in Wadaslintang Regency, Wonosobo, Central Java, Indonesia was built for five years, starting in 1983 and completed in 1987. In this study, the structure of the dam will be evaluated based on dynamic earthquake loading on the basis of the 2019 earthquake hazard map. Dynamic evaluation requires dynamic earthquake acceleration in the form of a time history of earthquake acceleration that is developed deterministically. The earthquake acceleration time history in this study was also developed based on earthquake acceleration from 2019 Indonesian Seismic Code (ISC). The earthquake ground motion for a sit can be generated deterministically or probabilistically. For the Wadaslintang dam (Figure 1) will evaluate the deformation of the dam structure based on dynamic earthquake loading.

Earthquake loading referred to here is earthquake ground motion in the form of a time history of acceleration (or it can be called just a time history). The time history is generated

deterministically. The time history can also be measured. The general form of the results of earthquake ground acceleration measurements can be seen in Figure 2. The time history of the measurement results is hereinafter referred to as the actual time history.



Figure 1. Wadaslintang Dam, Wonosobo, Central Java, Indonesia.

The actual time history will be used as a basis to generate a deterministic artificial time history through a spectral matching

process. The artificial time history will then be used to evaluate the structure of the Wadaslintang dam by looking at the response of the dam structure to its loading time history.

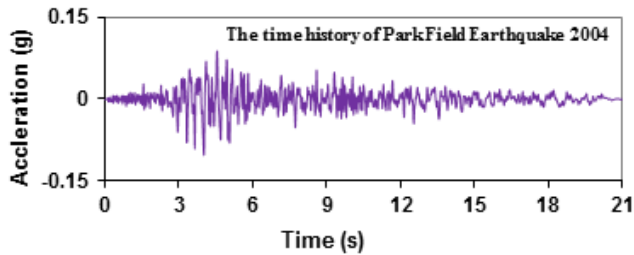


Figure 2. An example of the results of an earthquake ground acceleration measurement.

Studies related to the evaluation of high-rise building structures have been carried out by many experts. However, studies on evaluating dynamic dam structures have not been widely carried out in Indonesia. In general, the earthquake load used as the basis for evaluating a multi-story building structure is the vibration of earthquake waves in the form of a time history of earthquake acceleration. Time histories are usually developed by spectral matching procedures at bedrock or at ground level sites, Nicolaou [1]. Based on the procedure, the actual time history can be developed into two or more new time histories with the same or different frequency characteristics than the original time histories (the actual time histories). The new time history that is generated is called an artificial time history. The development of artificial time history with spectral matching procedure has been carried out by experts. Deterministically, Carlson *et al.* [2] altered the frequency characteristics of the suite of 28 ground motions before being used as input to a bilinear SDOF system. Ergun and Ates [3] transformed the frequency characteristics of the actual acceleration time histories to generate new time histories and compare the effects of near-fault ground motions on structures with far fault ground motions' effects. Wood and Hutchinson [4] selected ground motion using a probabilistic seismic hazard analysis and altered the frequency characteristics of the ground motion to certain target spectrum. Bayati and Soltani [5] have selected and changed the frequency characteristics of the ground motion deterministically for seismic design of RC frames against collapse. Pavel and Vacareanu [6] were selected actual acceleration time history using a probabilistic seismic hazard analysis and transform its frequency characteristics to appropriate spectrum to generate a new time history. Makrup and Jamal [7] changed the quantity of the earthquake ground motion by time history analysis (spectral matching procedure) to find new time history without alter its frequency characteristic. Makrup [8] developed design ground motion based on probabilistic seismic hazard analysis and code. In this case, earthquake wave propagation is also carried out from the bedrock to the surface to obtain a time history of acceleration at the ground surface. Makrup and Muntafi [9] generated the artificial ground motion for the Cities of Semarang and Solo Indonesia as basis to design and

evaluate the seismic risk for the multi stories building in the both cities. Irsyam, Hendriyawan, Dangkoa [10] developed the artificial earthquake acceleration time history to carry out seismic hazard assessment for Liquid Natural Gas storage tank terminal of the National Electrical Company (PLN) at Teluk Banten, Western Java, Indonesia.

A study related to the evaluation of the dam structure has been carried out by Wardani [11]. This study related to the impact of the 2010 earthquake hazard map of Indonesia on the stability of Kuiling dam slopes in Aceh province, Indonesia. The analysis also resulted in the safety factor of the dam slope based on the 2004 earthquake hazard map changing to a smaller one with the 2010 earthquake hazard map. The dam slope became unsafe. Putra [12] evaluated the slope stability of the Titab dam with a safety factor of more than 1 for several conditions. Tanjung [13] used the screening analysis method to evaluate the slopes stability of the embankment dam under the 2010 Indonesian earthquake load. The results of Tanjung's research showed that of the 80 dams studied, only 5 dams had a safety factor of more than 1 (safe slopes), the rest had a safety factor of less and equal than 1 (unsafe slopes). All of these studies used static earthquake loads to study slope stability and bending.

In this study, an evaluation of the structure of the Wadaslintang dam will be carried out using earthquake dynamic loads derived from the 2019 earthquake hazard map. This study will look at the overall response of the dam structure and then discuss and conclude it.

2. The Earthquake Wave

Earthquake waves referred to here are earthquake acceleration waves recorded at earthquake recording stations. Earthquake acceleration waves can also be developed by means of analysis using existing theories. To see the response of the dam structure as shown in Figure 3 to earthquake vibrations, a set of earthquake waves is needed, namely an earthquake acceleration time history at ground level. Time history is used as a basis for analyzing the response of the dam structure to determine the deformation of the dam structure due to earthquake loads.

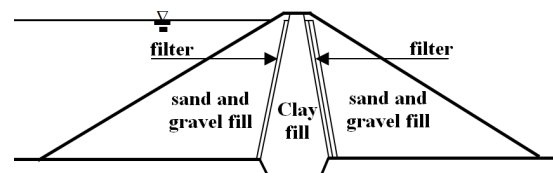


Figure 3. The standard form of the dam cross section of the rock fill type.

3. The Earthquake Load for the Dam

Calculation of earthquake loads is carried out by following construction and building guidelines and analysis of the stability of the embankment type dam due to earthquake loads, published by Ministry For the Public Works and Human Settlements, Indonesia (Pd T-14-204-A).

There are two views in determining earthquake loads

1. Operating basis earthquake, (OBE) is the earthquake with rocking limit in the ground surface on study location with 50% probability not exceedance in 100 years, which should be determined probabilistically. Dams and complementary buildings and their equipment must continue to function properly easy to repair, if the operating basis earthquake occurred, without taking into account the security review of human life.
2. Maximum design earthquake (MDE) is the earthquake that gives biggest shaking on the study location which used for design and analysis. For the dam that its collapse treats the life, so the maximum design earthquake should be taken at the same limits as CMCE to maintain the reservoir filling capacity. If the dam collapse is not life threatening, an earthquake smaller

than CMCE can be taken as MDE.

In the study, the two reviews above to determine the earthquake loads for a dam were not used, but the seismic load for the dam is calculated based on the seismic hazard map available at ISC (2019).

4. Design Response Spectrum

The research location point is at coordinates 7.607778° south; 109.831389° east. This point is right above the Wadaslintang dam body. If this point is plotted onto the ground shear wave velocity map (V_s^{30}) Figure 4, the V_s^{30} value will be obtained ranging from 350 to 750 m/s. It is assumed that V_s^{30} is equal to ± 360 m/s for the study point. Based on $V_s^{30} = 360$ m/s and Table 1 it is found that the soil site class at the Wadaslintang dam point is SC (very dense soil).

Table 1. Soil site classification.

Site Class	V_s	N	Su
A	>5000 ft/s	Not	not
Hard rock	>1500 m/s	Applicable	aplicable
B	2500 to 5000 ft/s	Not	not
Rock	760 to 1500 m/s	Applicable	aplicable
C	1200 to 2500 ft/s	>50	>2000 psf
Very dense soil and soft rock	370 to 760		>100 kPa
D	600 to 1200 ft/s	15 to 50	1000 to 2000 psf
Stiff soil	180 to 370 m/s		50 to 100 kPa
E	<600 ft/s	<15	<1000 psf
Soft soil	<180 m/s		<50 kPa
	Any profile with more than 10 ft (3 m) of soil having character		
	* Plasticity index $PI > 20$		
	* Moisture content, $w > 40\%$		
	* Undrained shear strength, $S_u < 500$ psf		
F	a. Soil vulnerable to potential failure or collapse		
Soil requiring the	b. Peats and/or highly organic clays		
site-specific	c. Very high plasticity clays		
Evaluation	d. Very thick soft/medium clays		

The design response spectrum was determined based on the Indonesian Seismic Code (ISC) 2019. The code provides earthquake hazard maps for the periods of 0.2 seconds and 1.0 seconds (see Figures 5 and 6). From Figure 5 is found the spectral acceleration for a 0.2 second period in the range of 0.6g to 0.7g. It is

assumed that the acceleration at the study point for a spectral period of 0.2 seconds is 0.65g or $S_s = 0.65g$. From Figure 6 is found the spectral acceleration for 1.0 second period in the range of 0.3g to 0.4g. It is assumed that the acceleration at the study point for spectral period 1.0 seconds is 0.35g or $S_1 = 0.35g$.

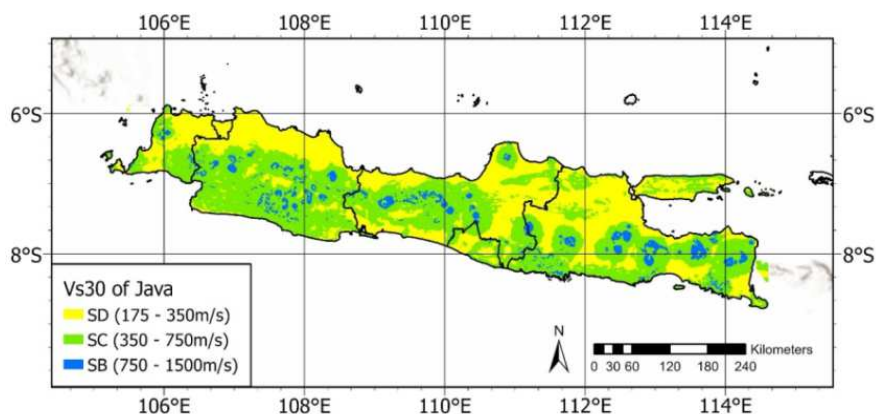


Figure 4. Soil site class (Muntafi 2021).

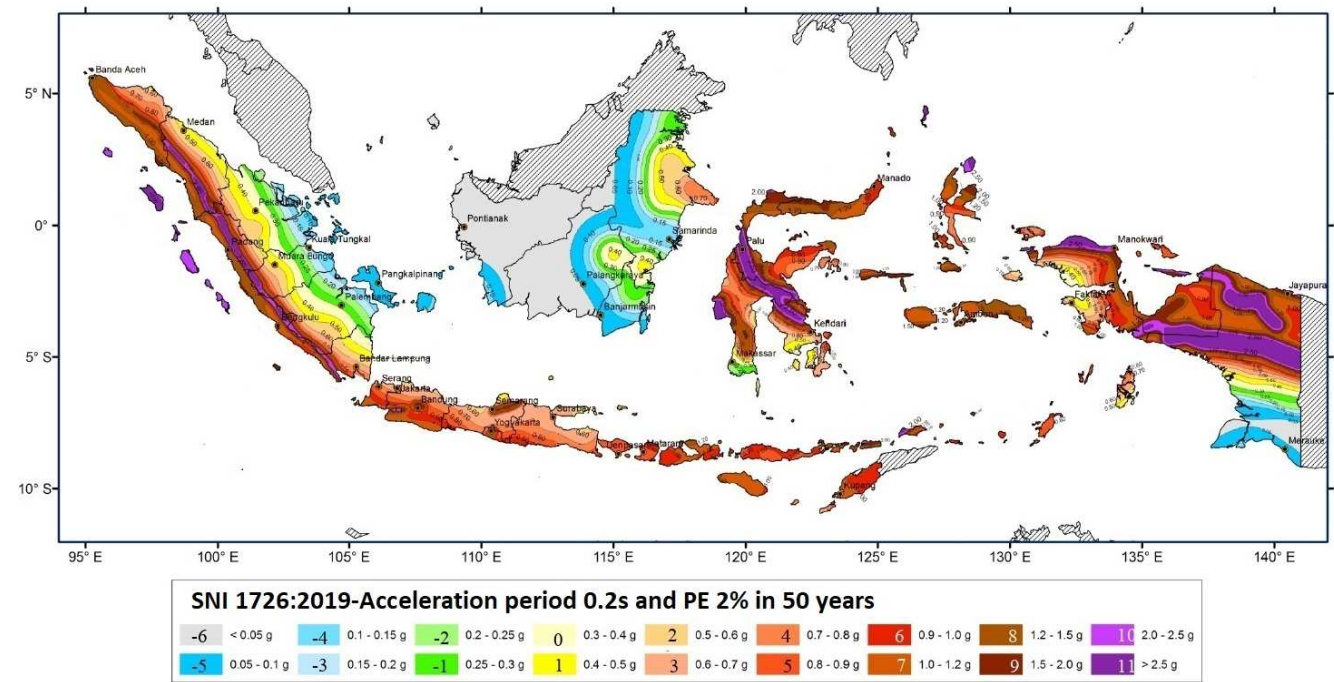


Figure 5. Seismic hazard map with spectral period 0.2 second, ISC (2019).

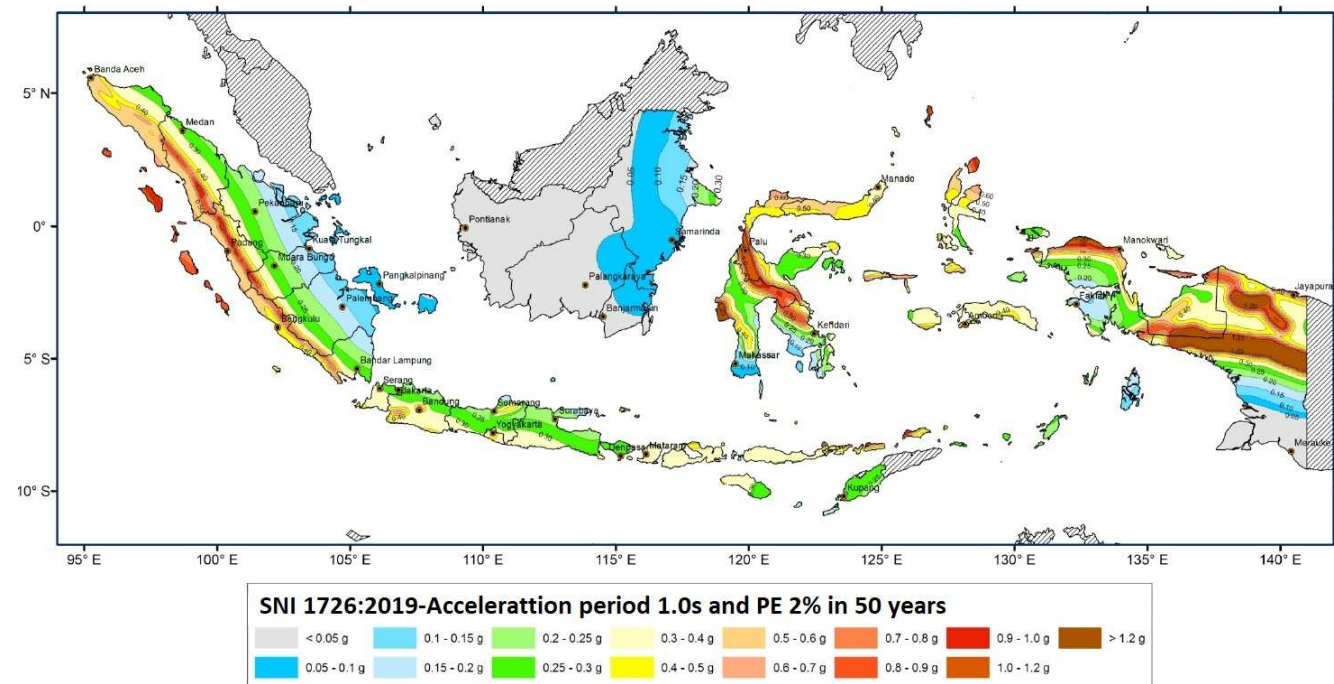


Figure 6. Seismic hazard map with spectral period 1.0 second, ISC (2019).

Table 2. Amplification factor for short period 0.2 second, (F_a).

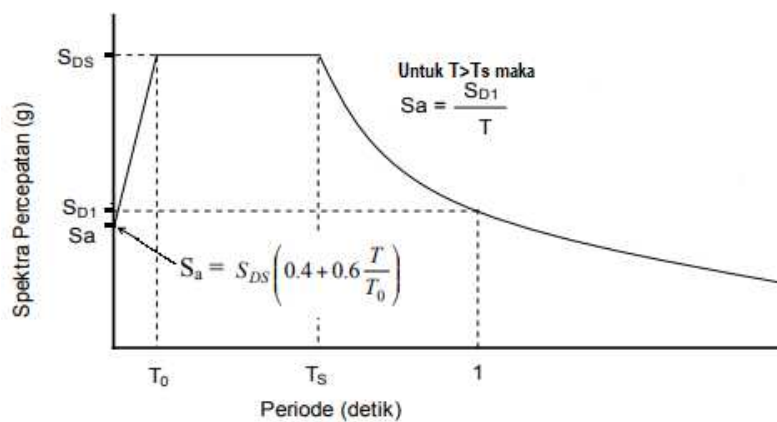
Class Site	Earthquake maximum acceleration response spectra parameters being considered targeted risk (MCE_R) mapped in short period, $T = 0.2$ second (S_s)					
	$S_s = 0.25$	$S_s = 0.50$	$S_s = 0.75$	$S_s = 1.00$	$S_s = 1.25$	$S_s = 1.5$
SA	0.8	0.8	0.8	0.8	0.8	0.8
SB	0.9	0.9	0.9	0.9	0.9	0.9
SC	1.3	1.3	1.2	1.2	1.2	1.2
SD	1.6	1.4	1.2	1.1	1.0	1.0
SE	2.4	1.7	1.3	1.1	0.9	0.8
SF			$S_s^{(a)}$			

Table 3. Amplification factor for long period 1.0 second, (F_v).

Class site	Earthquake maximum acceleration response spectra parameters being considered targeted risk (MCE_R) mapped in long period, $T = 1.0$ second (S_1)					
	$S_1 = 0.1$	$S_1 = 0.2$	$S_1 = 0.3$	$S_1 = 0.4$	$S_1 = 0.5$	$S_1 = 0.6$
SA	0.8	0.8	0.8	0.8	0.8	0.8
SB	0.8	0.8	0.8	0.8	0.8	0.8
SC	1.5	1.5	1.5	1.5	1.5	1.4
SD	2.4	2.2	2.0	1.9	1.8	1.7
SE	4.2	3.3	2.8	2.4	2.2	2.0
SF			$S_1^{(a)}$			

The parameter to determine the design response spectrum is the 2013 American Society of Civil Engineering (ASCE) code. The ASCE code is also used in ISC 2019. Furthermore, the design response spectrum parameters are determined based on Tables 2 and 3. To

determine the F_a value, it can be done by plotting the acceleration value of $S_s = 0.65g$ in Table 2 and to determine the F_v value it can be done by plotting the acceleration value of $S_1 = 0.35g$ in Table 3 related to the SC site class.

**Figure 7.** Design response spectrum (ASCE code 2013).

The standard form of 2013 ASCE code design response spectrum can be seen in Figure 7. The parameters in the figure can be calculated based on Equation (1), (2), (3), (4), (5), and (6).

The calculation starts by calculating S_{MS} and S_{DS} then calculating S_{M1} and S_{D1} .

$$S_{MS} = F_a S_s \quad (1)$$

$$S_{DS} = 2/3 S_{MS} \quad (2)$$

S_s is spectral acceleration and F_a is amplification factor for short period 0.2 second.

$$S_{M1} = F_v S_1 \quad (3)$$

$$S_{D1} = 2/3 S_{M1} \quad (4)$$

S_1 is spectral acceleration and F_v is amplification factor for long period 1.0 second.

$$T_s = S_{D1}/S_{DS} \quad (5)$$

$$T_0 = T_s/5 \quad (6)$$

T_s and T_0 are the spectral associated with the peak spectral acceleration.

The next will be developed the design response spectrum with $S_s = 0.65g$ and $S_1 = 0.35g$ have been found above.

Based on this S_s and S_1 , the results of the determination of the design response spectrum parameters for the research location points i.e. Islamic University of Indonesia hospital Bantul, Yogyakarta, Indonesia are as follows.

For $S_s = 0.65g$ and the soil site class is SC, from Table 2 we get $F_a = 1.28$;

For $S_1 = 0.35g$ and the soil site class is SC, from Table 3 we get $F_v = 1.95$.

Based on F_a and F_v , S_{MS} and S_{M1} are calculated using Equations (1) and (2). The result of the calculation is the S_{MS} and S_{M1} values below.

From equation (1) pound

$$S_{MS} = 1.28(0.65) = 0.83g$$

From equation (3) pound

$$S_{M1} = 1.95(0.35) = 0.6825g$$

Based on $\mu = 2/3$ (2013 ASCE code) can be calculated S_{DS} and S_{D1} . The result is as follows.

From equation (2)

$$S_{DS} = (2/3) 0.83 = 0.5547g$$

From equation (4) pound

$$S_{D1} = (2/3) 0.6825 = 0.455g$$

Based on the S_{DS} and S_{DI} values, the peak acceleration period T_S and T_0 can be calculated as below.

From equation (5) pound

$$T_S = 0.455/0.5547 = 0.82 \text{ s}$$

From equation (6) pound

$$T_0 = 0.82/5 = 0.164 \text{ s}$$

T_0 is the initial period of peak acceleration and T_S is the last period of peak acceleration. The results of the response spectra design images based on the computational parameters above can be seen in Figure 8. The response spectrum of Figure 8 was then defined as the target response spectrum to determine the artificial time history based on the spectral matching procedure and the actual time history of the selected earthquake.

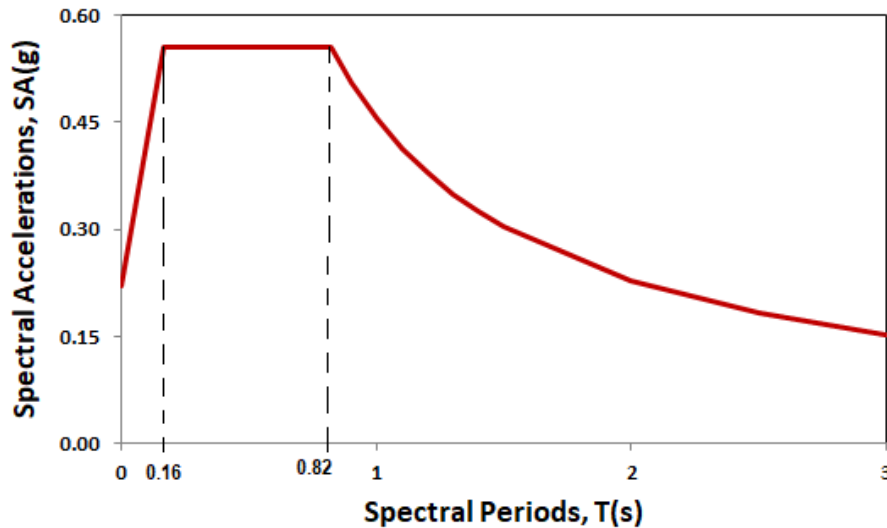


Figure 8. The results of determining the response spectrum design at the research site at ground level.

5. Time History Analysis

The time history referred to here is developing a new time history for the site being reviewed. Time history is developed based on recorded earthquake data from measurement results or is referred to as actual acceleration time history data of an earthquake and target spectrum data. Both data must be available on the same site. The procedure used to determine a new time history which is referred to as artificial time history is a spectral matching procedure. Spectral matching in the frequency domain will provide a new acceleration time history that has a frequency characteristic that is different from the actual time history frequency characteristic.

5.1. Select the Actual Time History

In this study the actual time history was selected based on a certain magnitude limit according to several parameters used in the study. On the other hand, the actual time history is also selected based on the type of soil in the study site. It is also assumed that the earthquake affecting the study point is a shallow crust earthquake. These are the three criteria as necessary conditions for selecting the actual time history from the earthquake catalog. Because this study uses an earthquake hazard map from the Indonesian Seismic Code (ISC) 2019 so it can be seen that the map developed is based on a magnitude range from $M = \pm 5$ to $M = \pm 7$ from shallow crust earthquakes. At the site, it is also known that the soil type is SC soil site class with V_s^{30}

ranging from 350 m/s to 750 m/s. Because the source of the earthquake is a shallow crustal, based on these criteria, it can be stated that the chosen earthquake to look for the actual time history is the 1971 San Fernando earthquake with $M = 6.61$ recorded at the Santa Felita Dam station with soil type is SC and $V_s^{30} = 389$ m/s. $M = 6.61$ is in the range of $M = \pm 5$ to $M = \pm 7$ and $V_s^{30} = 389$ m/s is in the range of 350 m/s to 750 m/s. So the San Fernando earthquake in 1971 is suitable to be used to find out the time history of earthquake and then the time history can be called as the actual time history. The time history of the 1971 San Fernando earthquake is shown in Figure 9.

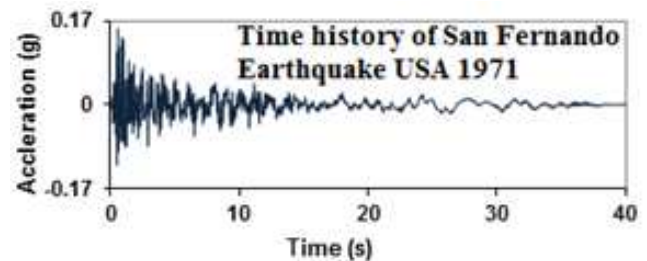


Figure 9. The time history of San Fernando earthquake USA 1971 at Santa Pelita Dam station.

5.2. Determination of the Actual Response Spectrum

The actual response spectrum from the time history of Figure 9 can be determined based on Equation (7).

$$m x'' + c x' + k x = -a_G \quad (7)$$

where, m is the mass, c is the damping, and k is the stiffness of the single degree of freedom system (SDOF). The results of the calculation of the actual response spectrum are in Figure 10.

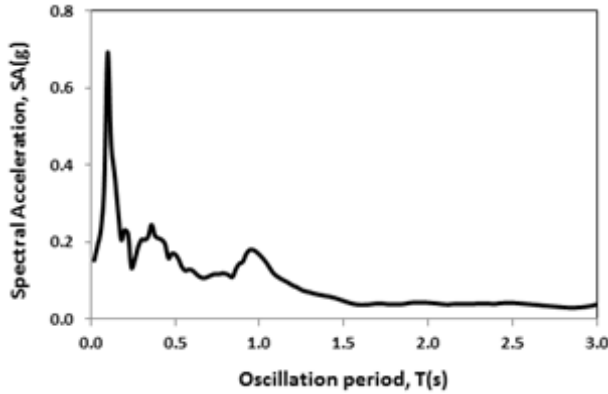


Figure 10. Actual response spectrum of the time history Figure 9.

5.3. Spectral Matching and Artificial Time History

To calculate the artificial time history, spectral matching procedure can be performed. The spectral matching procedure can be carried out based on the target spectrum as the matching objective and the actual response spectrum as the matched spectrum. The matching process can be performed in the frequency domain. The result of spectral matching is an artificial time history and a new response spectrum called the matching spectrum. The spectral matching procedure in the frequency domain according to Nicolaou [1] is:

- Select the target spectrum $\{S_a^{target}(T)\}$;
- Select the time history for match (TH_{aktual});
- Calculate the $\{S_a^{aktual}(T)\}$ actual response spectrum with the same attenuation as the target spectrum attenuation.
- Calculate the ratio of the actual spectrum and the target spectrum $\{SPR(T)\}$, see Equation (8).
- Calculate actual Fourier spectrum $\{F_{aktual}(\omega)\}$ from actual time history $\{TH_{aktual}(t)\}$ using discrete Fourier analysis algorithm (DFA);
- Use the frequency domain $SPR(\omega)$ in the form of Equation (9) to filter the actual Fourier series with the filtered Fourier filtered result $[F_{filtered}(\omega)]$ in the form of Equation (10).
- Calculate the time history with the frequency characteristics in step (f) using the Fourier inverse to find the TH(t) of the target spectrum.
- Calculate the mean error (deviation of the TH(t) response spectrum with respect to the target spectrum). If the calculation error in this step is allowed within the specified tolerance limits, the calculation is complete. If the error is not allowed then steps (b) to (h) are repeated until the error can be allowed.

$$SPR(T) = \frac{S_a^{target}(T)}{S_a^{aktual}(T)} \quad (8)$$

$$FILT(\omega) = \begin{cases} 1, & \omega < \omega_{min} \\ SPR(\omega), & \omega_{min} \leq \omega \leq \omega_{max} \\ 1, & \omega > \omega_{max} \end{cases} \quad (9)$$

$$F_{filtered}(\omega) = FILT(\omega) F_{aktual}(\omega) \quad (10)$$

where, T and ω are a spectral period (wave period) and cyclic frequency respectively. ω_{min} and ω_{max} are minimum dan maximum matching frequencies respectively.

Matching in the frequency domain, to estimate the error can be done as matching in the time domain. Therefore, the equation for estimating the error in the frequency domain is contained in Equation (11).

$$|Error|_N\% = 100 \sqrt{\frac{\int_{T_A}^{T_B} (S_a^{scaled} - S_a^{target})^2 dT}{\int_{T_A}^{T_B} S_a^{target} dT}} \quad (11)$$

where, $S_a^{scaled}(T)$ is the response spectrum of the actual time history $\{TH_{aktual}(t)\}$ generated by the spectral match in the frequency domain, and $S_a^{target}(T)$ is the target spectrum.

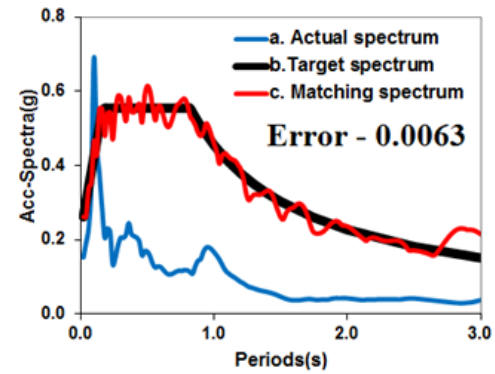


Figure 11. Spectral matching result of Figure 10 to Figure 8.

In the matching process in this case, the response spectrum of Figure 8 is set as the target spectrum and the response spectrum of Figure 10 as the actual response spectrum. The results of the spectral matching based on the above procedure are shown in Figure 11. Based on the results of the matching of Figure 11, it is found that the time history of the matching results is known as the artificial time history. Time history can be seen in Figure 12.

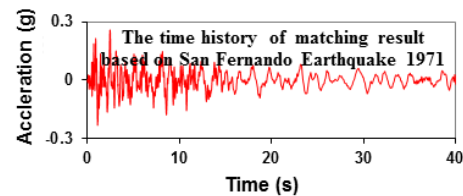


Figure 12. The artificial time history of a matching result.

If the time history of Figure 12 (artificial time history) is compared with Figure 9 (actual time history) it can be seen that the artificial time history has a larger amplitude than the actual time history, although the vibration pattern is not much different (see Figure 13).

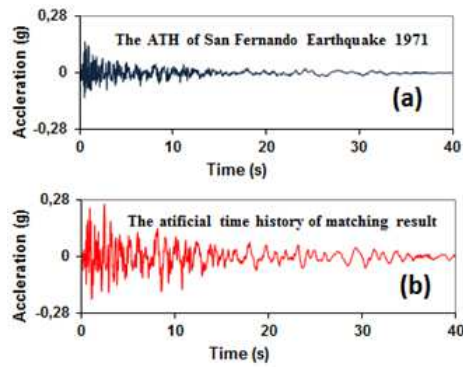


Figure 13. Time history aktual (a) dan artificial (b).

Therefore, it can be stated that the spectral matching in the frequency domain can change the frequency characteristics

from the actual time history to a new time history called artificial time history. Furthermore, the time history of Figure 12 will be used as a basis for conducting structural analysis of the dam to evaluate the deformation of the dam structure as a whole due to earthquake loads exerted on the dam.

6. Dynamic Response of the Dam Structure

Based on the dynamic analysis of the water structure published by the Ministry of Public Works of the Republic of Indonesia (2014), the dynamic analysis of the dam structure using a time history of earthquake acceleration can be carried out based on the water level in the dam reservoir. The normal water level of the reservoir is the main water level used in the analysis.

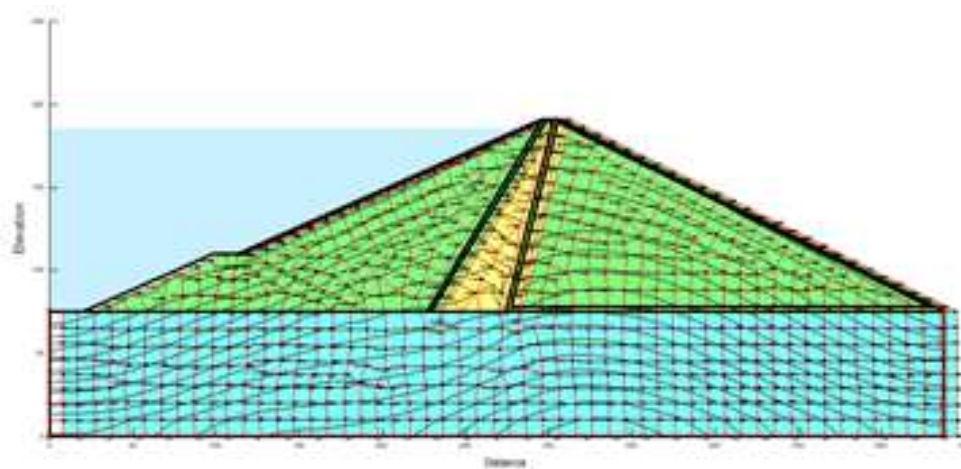


Figure 14. The dynamic response of the the Wadaslintang dam structure.

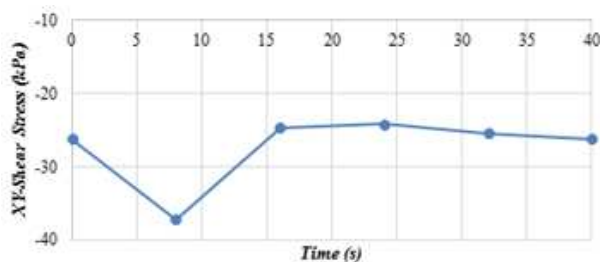


Figure 15. The total stress curve in relation to the time.

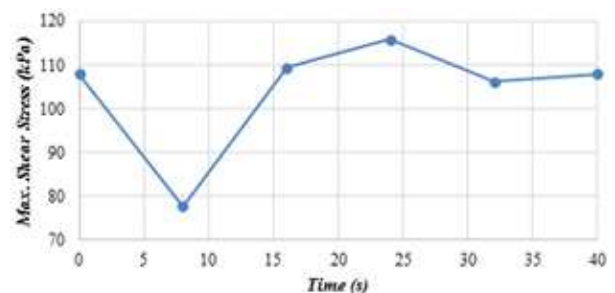


Figure 16. The shear stress curve in relation to the time.

Table 4. Soil layer parameters for deformation analysis.

No	Soil layer	Volume weight (KN/m ³)	V	Elasticity Modulus
1	Clay	18.83	0.30	9000
2	Filter	22.26	0.25	20000
3	Rockfill	21.18	0.30	80000
4	Rip-rap	21.18	0.27	140000
5	Foundation	22.26	0.30	20000

7. The Dam Structure Deformation

To determine the deformation of the Wadaslintang dam structure due to dynamic response, the GEOSTUDIO program with the SIGMA/W sub-program was used. Parameters inputted in the program are in Table 4.

The results of the structural deformation analysis of the Wadaslintang dam using the SIGMA/W sub-program can be seen in Figures 17 to 19.

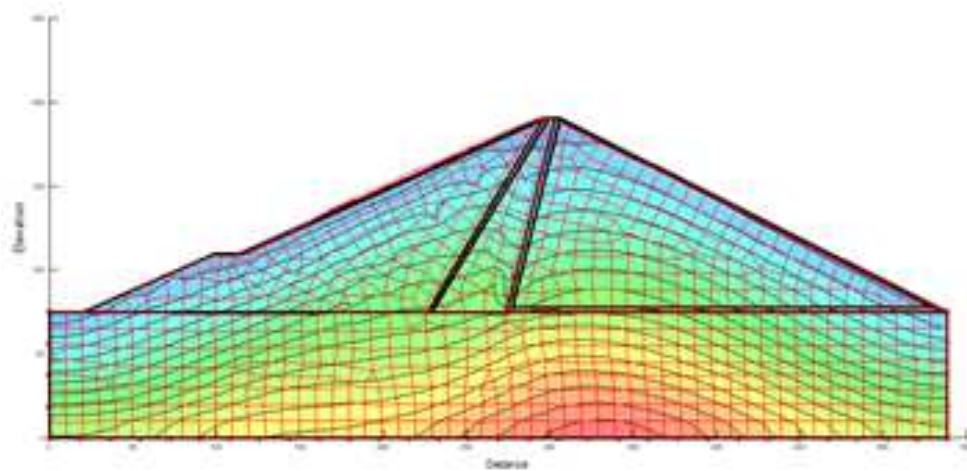


Figure 17. Deformation analysis result used SIGMA/W sub-program.

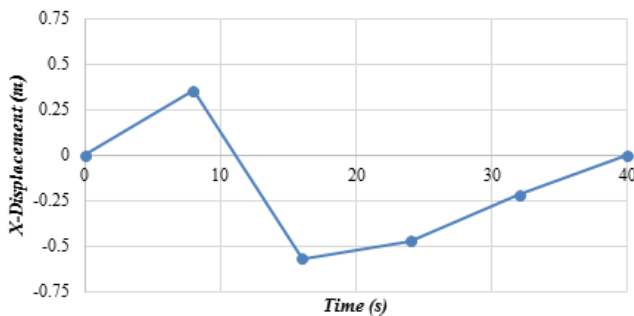


Figure 18. The deformation curve in the horizontal direction.

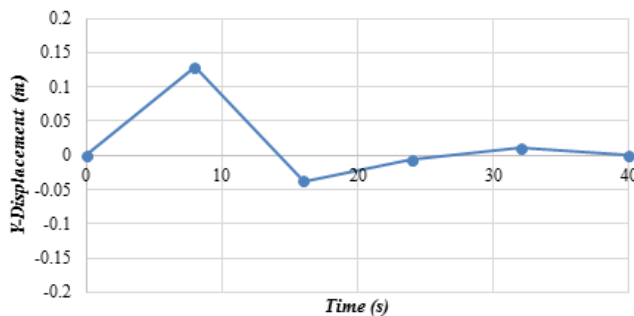


Figure 19. The deformation curve in the vertical direction.

8. Discussion

From the analysis carried out with the GEOSTUDIO program and the SIGMA/W sub-program and the QUAKE/W sub-program it was found that the total stress that occurs in the Wadaslintang dam structure is 37.16 kPa and the maximum shear stress that occurs is 282.07 kPa. The dynamic response of the dam greatly affects the level of deformation of the dam structure. The deformation that occurs at the top of the dam is actually a vertical permanent deformation. This deformation does not exceed 50% of the guard height and does not cause disturbances to downstream

stability, while the horizontal permanent deformation does not exceed 50% of filter thickness.

Based on the guard height data of the Wadaslintang dam, in half of the PMF (Maximum Flood Peak) discharge with guard height is 1.816 m, so that the deformation limit that can occur in the Wadaslintang dam structure is 0.906 m.

The thickness of the vertical filter on the Wadaslintang dam is 3.0 m, so the horizontal deformation limit that can occur is 1.5 m.

This limitation is to prevent the concentration of seepage in the dam structure which can initiate the occurrence of piping after the earthquake. The results of the structural deformation analysis of the Wadaslintang dam can be seen in Table 5.

Table 5. The deformation analysis result of the Wadaslintang dam structure.

No	Conditions	Result (m)	Requirement (m)	Status
1	Vertical Deformation	0.12	0.906	Safe
2	Horizontal Deformation	0.35	1.50	Safe

9. Conclusion

It has been produced the artificial earthquake acceleration time history on the ground surface in the research. The time history has been used to evaluate the Wadaslintang dam structure. From this evaluation was found that the dam structure stability to the shear process and rolling is safe, because the dam has the safe number greater than the conditions specified in the theory. The dam response to the time history of the earthquake wave that burden it show that the vertical and horizontal deformation (in meter) has the smaller deformation than the set requirement.

10. Recommendation

The dam structure which link to the earthquake vibration and the study of seismicity still much available opportunity

to make the research. As I have conducted the research about the dam evaluation due to the earthquake acceleration, so the evaluation of other dam or other structure deformation caused by the earthquake acceleration can be done by other researchers. For my colleague in civil engineering department, Islamic University of Indonesia can do the kind of research.

Acknowledgements

The author gratefully acknowledgement to head of Civil Engineering Department, Islamic University of Indonesia, that has supported this research in encouragement and funding.

References

- [1] Nicolaou. A. S. (1998), *A GIS Platform for Earthquake Risk Analysis*. A dissertation submitted to the Faculty of the Graduate School of State University of New York at Buffalo USA in partial fulfillment of the requirement for the degree of Doctor of Philosophy, August.
- [2] Carlson C. Pp., Zekkos D., McCormick J. P. (2014) Impact of time and frequency domain ground motion modification on the response of a SDOF system. *Earthquakes and Structures*, Volume 7, Issue 6, 2014, pp. 1283-1301.
- [3] Ergun M. and Ates S. (2013) Selecting and scaling ground motion time histories according to Eurocode 8 and ASCE 7-05, *Earthquakes and Structures*, Volume 5, Issue 2, 2013, pp. 129-142.
- [4] Wood, R. L., Hutchinson, T. C. (2012) Effects of ground motion scaling on nonlinear higher mode building response, *Earthquakes and Structures*, Volume 3, Issue 6, 2012, pp. 869-887.
- [5] Bayati Z, Soltani M. (2016) Ground motion selection and scaling for seismic design of RC frames against collapse. *Earthquakes and Structures*, Volume 11, Issue 3, 2016, pp. 445-459.
- [6] Pavel F., Vacareanu R. (2016) Scaling of ground motions from Vrancea (Romania) earthquakes. *Earthquakes and Structures*, Volume 11, Issue 3, 2016, pp. 505-516.
- [7] Makrup, L. and Jamal A. U., (2016). The Earthquake Ground Motion and Response Spectra Design for Sleman, Yogyakarta, Indonesia with Probabilistic Seismic Hazard Analysis and Spectral Matching in Time Domain, *American Journal of Civil Engineering*, 4 (6): 298-305.
- [8] Makrup, L. (2017) Generating Design Ground Motion by Probabilistic Seismic Hazard Analysis and Code, *EJGE (Electronic Journal of Geotechnical Engineering)*, Vol. 22, [2017] Bund. 5.
- [9] Makrup, L., and Muntafi, Y. (2016) Artificial Ground Motion for the Cities of Semarang and Solo Indonesia Generated Based on Probabilistic Seismic Hazard Analysis and Spectral Matching, *EJGE (Electronic Journal of Geotechnical Engineering)*, Vol. 21, [2016] Bund. 21.
- [10] Irsyam M., Hendriyawan, Dangkua, A. D (2003) Seismic Hazard Assessment LNG Storage Tank Terminal Teluk Banten, *Report of Seismic Hazard Study*, Bandung.
- [11] Wardani, T. (2014). *Pengaruh Penggunaan Peta Gempa 2010 Terhadap Analisis Dinamik Stabilitas Lereng Bendungan Keuliling Aceh*. Bandung: Universitas Komputer Indonesia.
- [12] Putra, T. G. (2016). Analisis Stabilitas Lereng Pada Bendungan Titab. *Jurnal Ilmiah Teknik Sipil Vol. 20 No. 1*, 13-14.
- [13] Tanjung, M. I. (2017). Screening Analysis Stabilitas Lereng Bendungan Urugan Akibat Gempa di Indonesia. *Jurnal Teknik Hidraulik Vol. 8 No. 1, Juni 2017*, 193-204.